A Novel Temporary Magnetic Remanence Thermodynamic Cycle

Remi Cornwall

Future Energy Research Group

Queen Mary, University of London, Mile End Road, London E1 4NS

http://webspace.qmul.ac.uk/rocornwall or http://vixra.org/author/remi_cornwall

Abstract

This paper presents a summary of research to utilise the massive amount of low grade heat energy, for instance which exists in the worlds oceans, by a new type of magnetic cycle. Developed herein are methods based on 2nd order phase changes that make it possible to achieve high efficiency despite small temperature differences with the reservoir. Ferrofluids displaying temporary magnetic remanence are an almost perfect embodiment of the working substance for these cycles. Standard Kinetic Theory, Thermodynamic and Electrodynamic analysis and experiment validates the new cycle.

1. Introduction

The impetus for magnetic heat engine research is the potential of having machines with few moving parts, high efficiency and low environmental impact.

Magnetic heat engines need a variation of magnetisation with temperature and two effects are noted: the force experienced by magnetic materials in an external field[1-3] ($\mathcal{M}$ is the volume magnetisation) and the magneto-caloric effect[4-7].

$$F = -\nabla\left(\mathcal{M} \cdot \mathbf{B}\right) \qquad \text{eqn. 1}$$
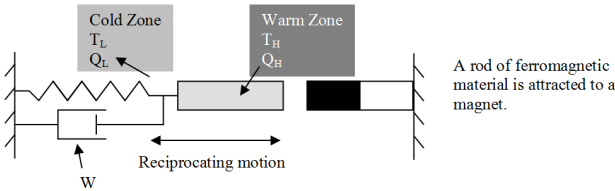

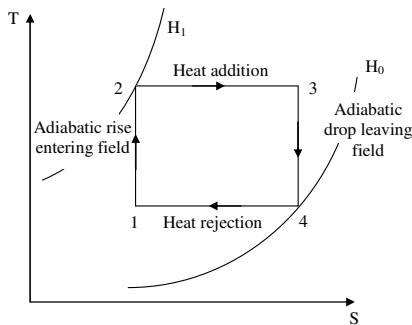
Figure 1 – A Simple Reciprocating Magnetic Motor

Figure 2 – T-S diagram, Magnetic Heat Engine

Figure 1 shows a means to convert heat energy to work by a simple reciprocating motor. A rod of ferromagnetic material is attracted to a magnet and does work against a spring. However at the same time near the magnet it is heated, absorbing heat Q_H, above its Curie temperature (the temperature above which the material becomes paramagnetic) with the result that its moment, $\mathcal{M}$, becomes smaller. Consequently the force on rod diminishes and it is retracted into the cold zone rejecting heat Q_L into the lower reservoir. Useful work is shown as being merely dissipated in the dashpot.

Thermodynamic analysis can be quickly performed by analysing this heat engine as two adiabatic processes alternated with isothermal processes (fig. 2). The Thermodynamic Identity equates the change in heat to the work around a cycle and thus the area on the T-S diagram is equivalent to multiplying the adiabatic temperature change on magnetisation by the isothermal change in entropy ([8] appendix 1),

$$(\Delta T)_S = -\frac{\mu_0 T}{C_H}\left(\frac{\partial \mathcal{M}}{\partial T}\right)_H \Delta H \qquad \text{eqn. 2}$$

$$\Delta S = -\mu_0\left(\frac{\partial \mathcal{M}}{\partial T}\right)_H \Delta H \qquad \text{eqn. 3}$$

Thus,

$$W = \int_{H_0}^{H_1} \frac{\mu_0 T}{C_H}\left(\frac{\partial \mathcal{M}}{\partial T}\right)_H dH \cdot \int_{H_0}^{H_1} \mu_0\left(\frac{\partial \mathcal{M}}{\partial T}\right)_H dH \qquad \text{eqn. 4}$$

Or approximately,

$$W \approx \frac{\mu_0^2 T}{C_H}\left(\frac{\partial \mathcal{M}}{\partial T}\right)_H^2 (\Delta H)^2 \qquad \text{eqn. 5}$$

The magneto-caloric effect (MCE) can also be used to refrigerate/pump heat and the MCE Carnot cycle's TS diagram is just the reverse of figure 2.
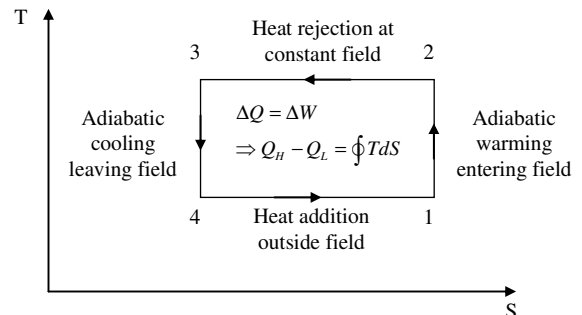

Figure 3 – T-S diagram MCE Carnot Refrigerator

1.1 The Limitation of MCE Carnot cycles

The heat engines discussed previously are more practically realised by heat transfer at constant magnetic intensity in the magnetic analogy of Brayton and Ericsson cycles[9] (figures 4 and 5). The former cycle performs heat transfer when the magnetic intensity is higher and thus achieves a higher temperature range and heat transfer between the magneto-caloric material and the heat transfer fluid. Figure 4 shows this as two adiabatic processes and two constant intensity processes. Process 2a-3 is an additional cooling caused by a regenerator that exchanges heat with process 4a-1. The Ericsson cycle heat pump features isothermal magnetisation and demagnetisation processes with regeneration at processes 2-3 and 4-1. Since the heat exchange process of regeneration in both cases requires a finite temperature difference, this is an irreversible process and so is a decrease in the efficiency of both cycles compared to the Carnot cycle.
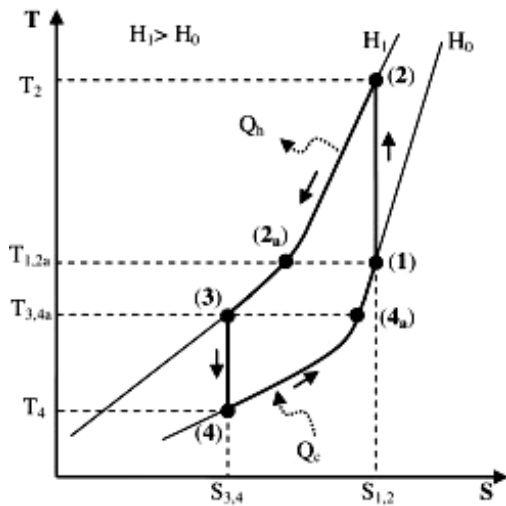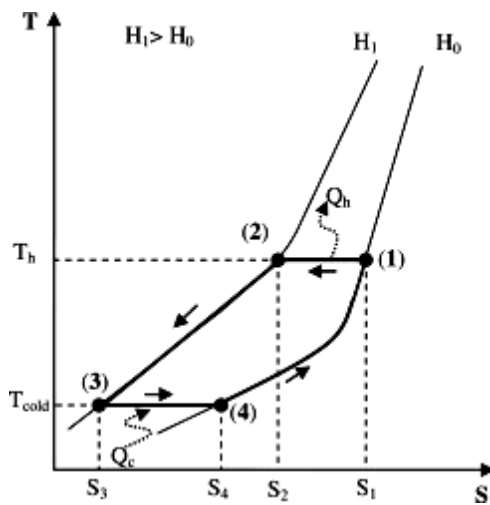

Figure 4 – Magnetic Brayton cycle

Figure 5 – Magnetic Ericsson cycle

Cornwall[8] and Gschneidner et-al[9] go into more detail about cascade Ericcson and the Active Magnetic Regeneration cycle but what is important to the research community is improving the magneto-caloric effect at the core of these cycles. A number of desirable material features are listed[9, 10]:

- Low Debye temperature[11].
- Curie temperature near working temperature.
- Large temperature difference in the vicinity of the phase transition.
- No thermal or magnetic hysteresis to enable high operating frequency and consequently a large cooling effect.
- Low specific heat and high thermal conductivity.
- High electrical resistance to avoid Eddy currents.

Gadolinium alloys and Lanthanum-Iron-Colbalt-Silicon alloys, $La(Fe_{1-x}Co_x)_{11.9}Si_{1.1}$ with their "giant magneto-caloric effect" are the focus for materials research due to their inherent high MCE although traditional ferromagnetic materials enter the scene again in the form of colloidal suspensions called ferrofluids.

We present now a new type of cycle based upon a feature of so-called super-paramagnetic materials called Temporary Remanence, unused in current heat engines, that has a wide temperature range of operation by being able to boost (eqn. 15) the MCE effect by a phenomenon called "dipole-work" (eqn. 6, Cornwall[8], fig. 9 and sec. 2.3).

$$W_{dw} = \int_{M,V} \mu_0 M dM \cdot dV = \frac{1}{2} \mu_0 M^2 V \quad \text{eqn. 6}$$

This dipole-work leads to an extra term on the thermodynamic identity and is related to the Faraday Law collapse of the temporary magnetic flux generating power into a resistive load. This can be made greater than the magnetisation energy input,

$$E_{mag} = \int_{M,V} \mu_0 H dM \cdot dV = \mu_0 H M V \quad \text{eqn. 7}$$

The difference come from the heat energy converted (secs. 2.1 and 2.2) into work. Thus the heat engine generates electrical power directly and also cools.

2. Detail on the Temporary Remanence Cycle

In our research we use a stable nanoscopic suspension of magnetic particles in a carrier fluid

called ferrofluid[7]. The particles are so small that they are jostled continuously by the Brownian motion. As a consequence they on magnetisation display "super-paramagnetism"[5, 7, 12] which on the spectrum from diamagnetism to anti-ferro/ferrimagnetism to paramagnetism to ferri/ferromagnetism, displays properties similar to both paramagnetism and ferri/ferromagnetism: they display no permanent remanence but are somewhat easy to saturate compared to paramagnets due to their large spin moment. Temporary remanence is manifest by two mechanisms:

$$\text{Néel:} \quad \tau_N = \frac{1}{f_0} e^{\frac{KV}{kT}} \qquad \text{eqn. 8}$$

And

$$\text{Brownian:} \quad \tau_B = \frac{3V\eta_0}{kT} \qquad \text{eqn. 9}$$

The first relaxation rate can be understood as internal to the ferrofluid particle and involves lattice vibration and hence it contains the energy term KV related to the crystalline anisotropy constant and the volume of the particle. The latter is related to the jostling of the particle by the suspending fluid and contains an energy term related to the viscosity of the suspending fluid and the volume. Nature uses the principle of least time to determine which dominates the relaxation rate. Obviously these quantities are amenable to engineering.

Another feature they display on rapid magnetic cycling is hysteresis loss[13, 14]. This is most pronounced if the rate of magnetisation is comparable to the relaxation rate. The phenomenon is directly related to the Fluctuation-Dissipation Theorem.[15].
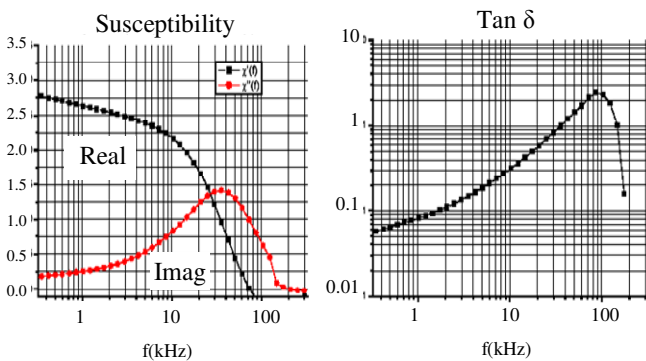

Figure 6 – Hysteresis loss in typical ferrofluid
(Courtesy Sustech Gmbh)
LHS Bodé plot in and out-phase components
RHS: Power loss angle

The cycle (called a micro-cycle) is implemented as a magnetising step followed by a de-magnetising step:
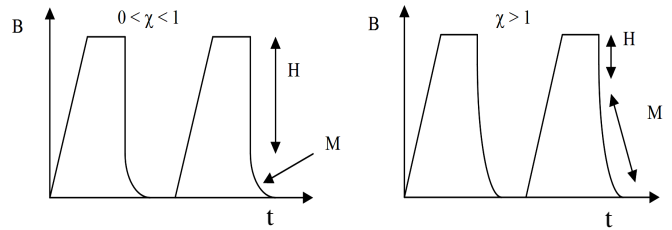

Figure 7 – *Micro-cycle* magnetising pulses
for 0 < χ< 1 and then χ> 1

The figure above shows a train of magnetising pulses for two cases, small and large susceptibility[5]. Observe how the switch-on phase is slow, so that significant hysteresis loss isn't incurred and the switch-off is abrupt to leave a temporary remnant flux (the "Independent Flux Criterion" sec. 2.3.1). Micro-cycles are completed many times a second and result in an adiabatic cooling of the ferrofluid working substance.

To complete the heat engine, the working substance needs to be placed in contact with an external (albeit only one) reservoir. The plant diagram or macro-cycle is depicted in the next figure. In this figure, the micro-cycles happen many times as the working substance transits the "power extraction area" A-B.

For the purposes of argument, let us dispel concerns about the pressure-volume work that must be expended circulating the fluid against its tendency to be drawn into the magnetised power extraction area by saying there is a portion of the operation when the magnetising fields are switched off and fluid is simply pumped further around to the heat exchange area C-D.
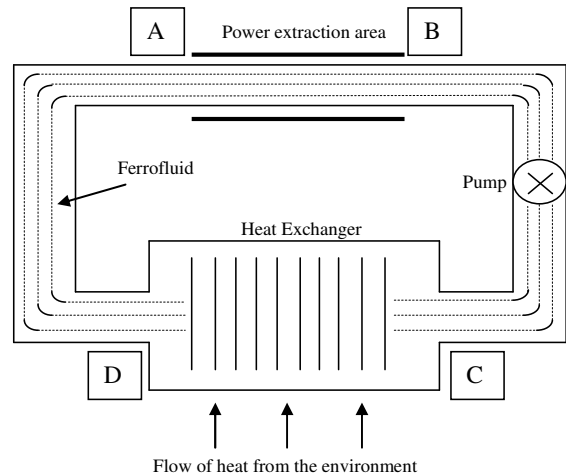

Figure 8 – Plant Diagram (*Macro-cycle*)

We shall develop the theory of the temporary remanence (TR) cycle heat engine by three intersecting analyses: Kinetic Theory, Thermodynamic and Electrodynamic Theories.

2.1 Kinetic Theory

In the thesis[8] a lattice of magnetic dipoles is set up to model the ferrofluid (fig. 9).

N.B. this is not just an inductor in a magnetise-demagnetise cycle but it is able to do excess work into the electrical load R (Independent Flux Criterion)
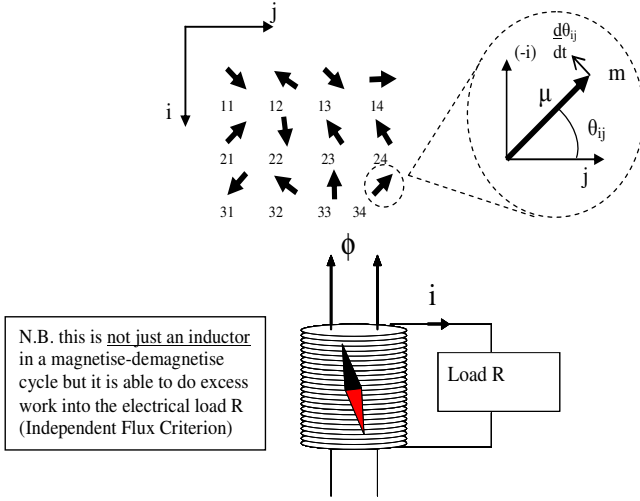
Figure 9 – The Kinetic Theory Model

The model of dipole-dipole interactions leads to the angular acceleration of each dipole:

$$\ddot{\theta}_{ij} = \frac{1}{I}\left(-k_{dip} \sum_{\substack{ii=i-1, \\ jj=j-1 \\ ii\neq i \wedge jj\neq j}}^{\substack{ii=i+1 \\ jj=j+1}} \tau\left(\theta_{i,j}, \theta_{ii,jj}, \mathbf{m}, \mathbf{r}\right) - \mathbf{m}_{ij} \times \mathbf{B}_{ext} \right) \quad \text{eqn. 10}$$

The torque experienced by each dipole is from the external field of the solenoid (B_{ext}) and the dipole-dipole interactions resulting from the local fields of its neighbours:

$$\tau\left(\theta_{ij}, \theta_{ii,jj}, \mathbf{m}, \mathbf{r}\right) = -\mathbf{m}_{ij} \times \overline{\mathbf{B}_{local.neighbour}} \quad \text{eqn. 11}$$

Taken as a bulk effect, this is of the form const x MdM or the dipole-work[8] (eqn. 6) where $B = \mu_0 M$

The model can be run as a molecular dynamics simulation and the author attempted this to good success, apart from the lack of convergence or *Energy Drift* in these type of simulations from use of non-sympletic algorithms[16]. It wasn't thought worthwhile to pursue this further when, as we shall see, analytical solution exists. Netheretheless the entropies of position and velocity and the temperature are calculated:

$$S_{pos} = const \times \ln\left(\text{standard deviation } \theta_{ij}\right)$$
$$S_{vel} = const \times \ln\left(\text{standard deviation } \dot{\theta}_{ij}\right) \quad \text{eqn. 12}$$
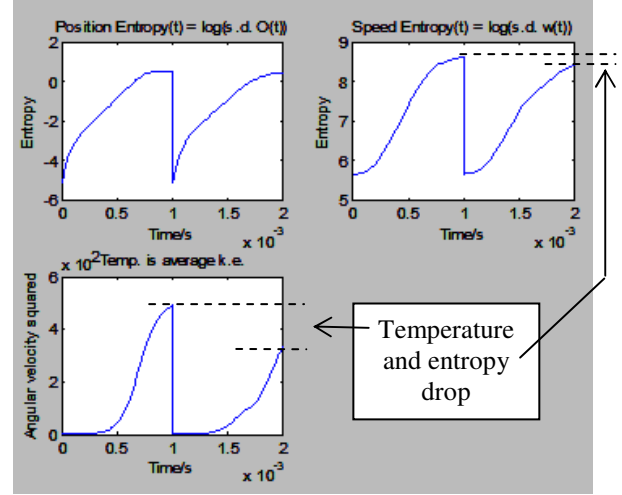$$T = const \times \text{average}\left(\dot{\theta}_{ij}^2\right)$$

Figure 10 – Relaxing to equilibrium and then the same but with dipole-work

Two simulations were performed, one after the other: In the first simulation the dipoles were all aligned at the start with zero kinetic energy. The simulation shows this "relaxing" to a random orientation (the position entropy increases). The potential energy at the start is converted into random kinetic energy (hence the temperature rises as does the velocity entropy).

The second simulation following right after for comparison models relaxation with dipole-work, that is, the assembly generates electrical work which leaves the system and gets dumped into the resistive load.

An analytical solution[8] can be obtained by the statistical averaging of the ensemble eqn. 10:

$$I\ddot{\theta}_{ij} = -k_v m_{ij} \sum_{ii,jj} \frac{\partial}{\partial t}\left(m_{ii,jj}\cos\theta_{ii,jj}\right)\sin\theta_{ij} \rightarrow I\ddot{\theta}_{ij} = -k_v\left(m_{ij}\sin\theta_{ij}\right)^2 \dot{\theta}_{ij}$$

eqn. 13

Thus each dipole experiences a drag force (hence proportional to the angular velocity $\dot{\theta}_{ij}$) and slows (hence both temperature and entropy decrease) and this is directly related to the dipole-work (eqn. 11). This shows the mechanism for the transduction of heat energy from the working substance to the electrical load.

Kinetic Theory/Statistical Mechanics is the source of the Boltzmann expressions in equations 8 and 9. Anisotropy can be added to the model (eqn. 10) such that rotation cannot occur unless an energy barrier is exceeded. This has the obvious effect of slowing down the relaxation rate. It is shown ([8] section 2.1.3) that compared to the intrinsic anisotropy energy barrier for the ferrofluid, the additional energy barrier from the dipole-work is

entirely negligible, thus kinetically the process of the magnetise-demagnetise TR cycle occurs.

2.2 Thermodynamics

The relation between Kinetic Theory, Statistical Mechanics and Thermodynamics is close. The first is a low-level description of single microscopic entities acting in concert; the next is a statistical description of a multitude of these low-level equations; finally thermodynamics relates bulk properties to average properties predicted by Statistical Mechanics.

To be a heat engine, the working substance must first have a property that is a strong function of temperature. This is immediately apparent in equations 8 and 9 with ferrofluid. However with conventional magneto-caloric effect (MCE) engines, focus dwells upon the paramagnetic-ferromagnetic transition and the Curie Point[5, 8]. In the author's thesis a link is made between the TR cycle (figures 7 and 8) and conventional MCE engines by the thermodynamic identity:

$$dU = TdS + \mu_0 H d\mathcal{M} + \mu_0 M d\mathcal{M} \qquad \text{eqn. 14}$$

The last term is the dipole-work such that an amended delta-T equation is derivable by considering 2nd cross-derivatives ([8] section 2.2 and appendix 1) related to the change in magnetising field *and* remnant magnetisation:

$$\Delta T = -\mu_0 \frac{T}{C_H} \left(\frac{\partial \mathcal{M}}{\partial T} \right)_H \left[\Delta H + \Delta M_{rem} \right] \qquad \text{eqn. 15}$$
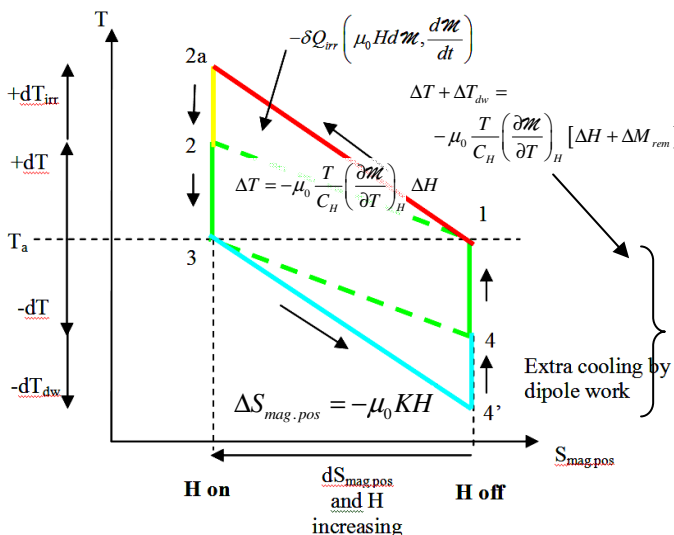

Figure 11 – Temperature- Positional Entropy Diagram for the micro-cycle
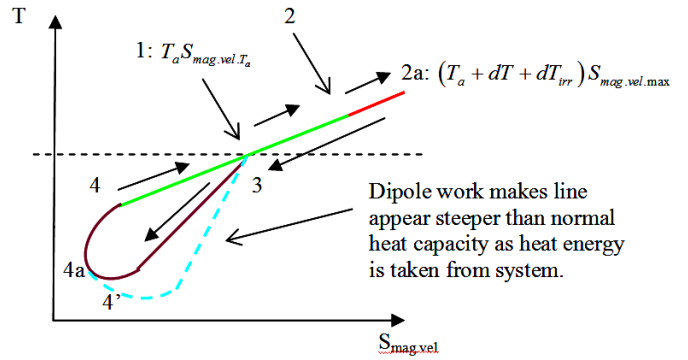

Figure 12 – Temperature- Velocity Entropy Diagram for the micro-cycle

This shows that, unlike conventional MCE cycles the TR cycle can operate below the Curie point (so that ΔT on magnetisation from ΔH is negligible) because the magneto-caloric effect occurs from the new dipole-work term in equation 14. Also we point out that, although ΔT is small, the immense surface area of nanoscopic magnetic particles in contact with the ferrofluid carrier liquid ensures massive heat flow ([8] section 2.2.3).

It is possible to construct ([8] section 2.2.1 to 2.2.4) a temperature-entropy diagram for the micro and macro-cycles (figs. 11 and 12). The figures depict temperature entropy diagrams for an infinitesimal TR cycle. They are somewhat of an abstraction in that the cycle places the magnetic component of the ferrofluid in contact with the carrier fluid at set points in the cycle (2-3) and (4, 4'-1) and considers them thermally isolated for the rest, whereas in reality the magnetic and fluid systems are always in intimate thermal contact. Thermodynamics requires one to construct a series of states with discernable, stable thermodynamic parameters and this is difficult when the system passes through a series of meta-states.

Figure 11 depicts positional entropy which directly related to magnetic ordering hence the magnetic field of the working substance. The internal cycle represented by numbers 1-4 is the simple MCE in contact with a reservoir. The field switches on between 1 and 2 with the temperature of the working substance raising as the heat capacity is lowered by the magnetising field (the magnetic heat capacity falls and heat is repartitioned to mechanical/kinetic part of the system). Between 2-3 the magnetic system is placed in contact with the ferrofluid carrier liquid which acts as a virtual reservoir and heat is rejected to it. Then between 3-4 the magnetic part, isolated once again, has the magnetising field switched off whereupon the heat capacity rises and heat flows from the mechanical part of the heat capacity to the magnetic part once again such that the magnetic system drops below

T_a, the temperature of the carrier fluid. On step 1-4, the magnetic system is placed in contact with the fluid reservoir and heat flows from it to the magnetic system.

The TR cycle is an adjunct to the reversible MCE cycle in contact with an external reservoir at points 1-2a-2, which represents hysteresis heating of the magnetic component and 3-4'-4, which represents the extra cooling by dipole-work.

The step numbers correspond similarly the T-S diagram for the mechanical part of the heat capacity of the magnetic system (fig. 12). We see that it is once again based on the reversible MCE cycle in contact with an external reservoir at steps 1-2-3-4. The difference occurs at point 2-2a with the hysteresis heating (and hence heat transfer between 1-2 on figure 11) and dipole-work cooling 3-4'-4 and heat transfer on figure 11 between 4'-4-1.

One further point is the conversion of the magnetisation energy (eqn. 7) into internal energy as the magnetising field is switched off at point 3-4. This is shown as an extra heat input 3-4a-1 in the diagram below and in figure 12 as steps 3-4'-4a-4-1.
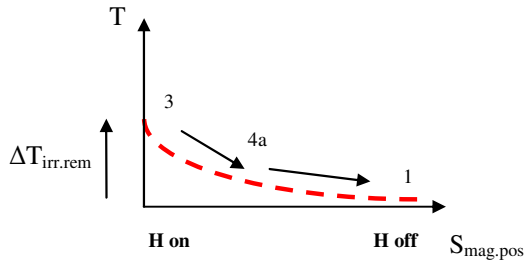
Figure 13 – The magnetising energy becomes internal energy

The consideration of these diagrams([8] appendices 6 and 7) allows the development of the energy balance equation:

$$-C_H \frac{d}{dt}\left(T_{mechanical}\right) = \frac{d}{dt}\left(Q_{external}\right) - \frac{d}{dt}\left(W\right) + \frac{d}{dt}\left(W_{irreversible}\right) \quad = 0$$

eqn. 16

This states the obvious really, that the internal energy is dependent on the heat dumped into the ferrofluid minus the dipole-work.

Overall the combined T-S diagram for the positional and mechanical entropies of the working substance is shown in figure 14. Once again, at its core is the reversible MCE cycle 1-2-3-4.
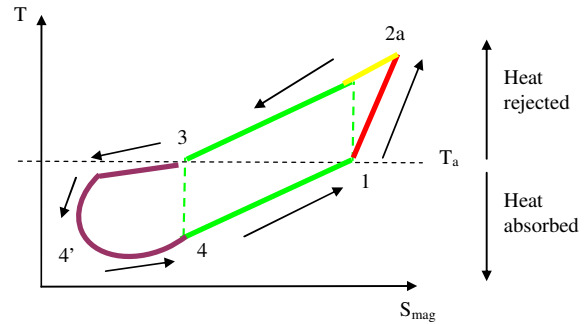
Figure 14 – Temperature-Entropy diagram for the Microcycle Composed of the positional and velocity T-S diagrams sub-cycles

As mentioned in the discussion about the plant diagram (fig. 8), the macro-cycle is made from many concatenated micro-cycles in the power extraction area. The micro-cycles cause the adiabatic cooling (if we neglect hysteresis heat inputs) of the ferrofluid working substance and we arrive at figure 15 (see [8] section 2.2.4 for original figure).
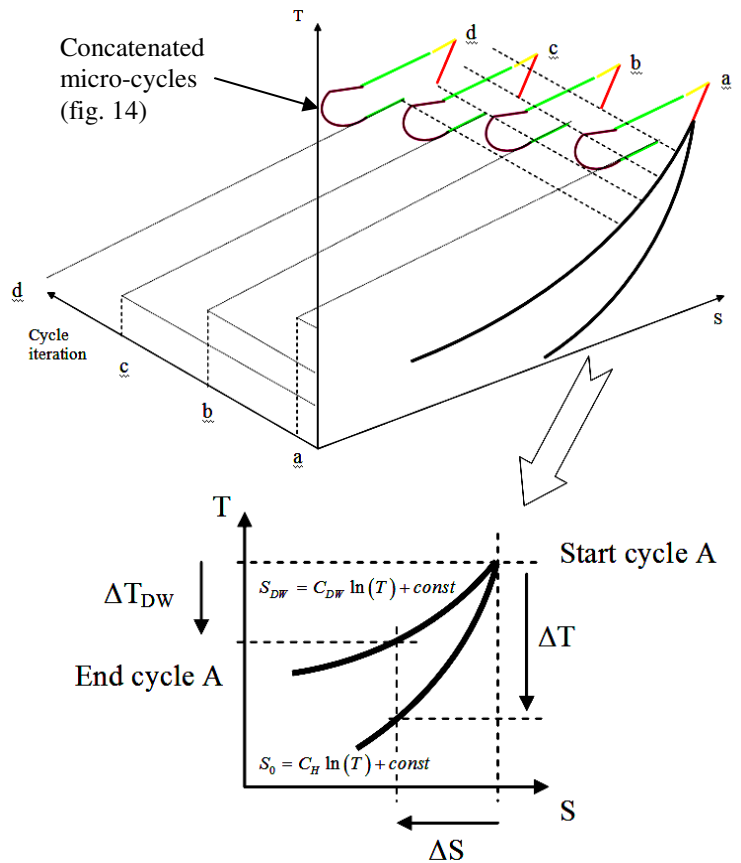
Figure 15 – How Micro-cycles relate to the Macro-cycle on a T-S diagram

The 2nd order phase change and the dipole-work in the thermodynamic identity make the working substance (eqn. 14) seem like another substance (more of this later in the discussion) with a higher

heat capacity. In the lower sub-figure of figure 15 the dipole-work causes a temperature drop ΔT_{DW} for entropy change ΔS as heat energy leaves the system. If we reverse our direction and go up the up trace and imagine we are warming the virtual substance, heat energy not only goes to the working substance but to the external system because of the dipole-work. In comparison the "native" heat capacity of the working substance without the dipole work in lower trace of the sub-figure is:

$$S_0 = C_H \ln(T) + const \qquad \text{eqn. 17}$$

The upper trace has an higher virtual heat capacity:

$$S_{DW} = C_{DW} \ln(T) + const \qquad \text{eqn. 18}$$

Zooming out from the upper sub-figure of figure 15 we arrive at the macro-cycle T-S diagram and then relate that to the plant diagram of figure 8 by the labels A-B-C-D:
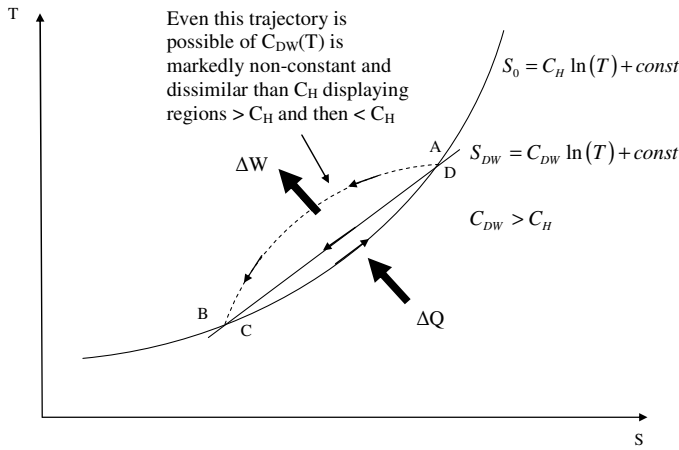

Figure 16 – Macro-cycle T-S diagram related to points on plant diagram

The area between the two trajectories of heat capacity C_H (eqn. 17) and C_{DW} (eqn. 18) is the heat absorbed at the heat exchanger and converted into electrical energy in the power extraction zone.

2.3 Electrodynamics

The Kinetic Theory and Thermodynamic analysis of the previous section have laid the groundwork for the TR cycle. It would seem a simple matter of Faraday/Lenz law collapse of the remnant flux in to a coil attached to an electrical load to deliver the goods of heat energy conversion, as depicted in figure 9. However there is some subtlety in the explanation of the demagnetisation step and a final electrical method to deliver excess power.

2.3.1. Not "just an inductor"

The lower sub-figure in figure 9 and the magnetise-de-magnetise cycle creates the impression that the setup is just a simple electrical circuit and if anything, should act as a dissipative sink of energy due to hysteresis losses. We show that this is not so and that excess electrical energy can enter the circuit from an external source of mechanical "shaft-work", effectively rotating the source of the magnetic flux inside the coil.

Firstly we consider the net electrical work around a magnetisation, de-magnetisation cycle.

$$\oint vi\, dt = -\oint \frac{d\lambda}{dt} i\, dt \qquad \text{eqn. 19}$$

Where λ is the flux linkage. Integrating the RHS by parts:

$$\oint i(t) \frac{d\lambda(t)}{dt} dt = \left[i(t)\lambda(t) - \int \lambda(t) \frac{di(t)}{dt} dt \right]_{0^+}^{0^-}$$

$$= i(0^-)\lambda(0^-) - i(0^+)\lambda(0^+) - F\left(\lambda(0^-), i(0^-)\right) + F\left(\lambda(0^+), i(0^+)\right)$$
$$\text{eqn. 20}$$

Where F(..) is the integrand of the parts term. Now, since $i(0^+) = i(0^-)$ and $\lambda(0^+) = \lambda(0^-)$ the first two terms cancel. Let a dependent flux be represented by,

$$i(t) = g\left(\lambda(t)\right) \qquad \text{eqn. 21}$$

Where g is an arbitrary function. The second integral of eqn. 20 can be integrated by parts a second time by applying the chain rule:

$$\int \lambda(t) \frac{di(t)}{dt} dt = \int \lambda(t) \frac{dg\left(\lambda(t)\right)}{d\lambda(t)} \frac{d\lambda(t)}{dt} dt \quad \text{eqn. 22}$$

Thus,

$$\oint \lambda(t) \frac{dg\left(\lambda(t)\right)}{d\lambda(t)} d\lambda(t) = \left[\lambda(t) g\left(\lambda(t)\right) - \int g\left(\lambda(t)\right) \cdot 1 \cdot d\lambda(t) \right]_{0^+}^{0^-}$$

$$\Rightarrow G\left(\lambda(0^+)\right) - G\left(\lambda(0^-)\right) = 0$$
$$\text{eqn. 23}$$

The first term on the RHS cancels due to the flux being the same at the start and end of the cycle. The integrand on the RHS cancels for the same reason. The above result shows that a dependent flux (eqn. 21) cannot lead to net power. The proof sheds more light on the necessary condition for an independent flux: *the flux is constant for any current including zero current* – it bares no relation to the modulations of the current. The proof also dispels any form of dependent relation, non-linear or even a delayed effect. If equation 21 was

$i(t) = g\left(\varphi(t-n)\right)$ this could be expanded as a Taylor series about g(φ(t)) but there would still be a relation, the flux would still be dependent.

Thus it is a statement of the obvious (the First Law of Thermodynamics) that excess power production in an electrical circuit cannot happen by electrical means alone; flux changes must happen by some <u>outside agency</u> such as electro-mechanical shaft-work to cause energy transduction.

In regard to the Kinetic Theory section and figure 9, we are drawing an analogy with the microscopic dipoles rotating via the randomisation process and the "micro-shaftwork" of heat energy. In fact, considering the energy of a dipole in a field[1-3]:

$$E = +\mathcal{M} \cdot \mathbf{B} + const \qquad \text{eqn. 24}$$

It matters not whether the magnetic moment is rotated wholesale or randomised between the maximum and minimum energy configuration, it is the same result:

$$\Delta E\big|_{max}^{min} = \mathcal{M}B\cos\theta\big|_0^{\pi/2} \text{ or } \mathcal{M}\big|_{\mu_{max}}^0 B\cos\theta \quad \text{eqn. 25}$$

2.3.2. Simple resistive load returns less than the input magnetisation energy

We can model the electrodynamics of the de-magnetisation step into a resistive load by a set of state equations[8]:

$$\frac{dM}{dt} = -\frac{1}{\tau}\left(M - \chi\mu_r H\right) \qquad \text{eqn. 26}$$

$$-\frac{d\lambda}{dt} - iR = 0 \qquad \text{eqn. 27}$$

Where,

$$H = \frac{N}{D}i \qquad \text{eqn. 28}$$

And

$$\lambda = NAB \Rightarrow NA\mu_0\mu_r\left(H + M\right) \qquad \text{eqn. 29}$$

Equation 26 represents very accurately[5, 7, 13, 14] the dynamics of the ferrofluid to a magnetising field, H[†]. The "effective susceptibility" $\chi\mu_r$ is just the product of the susceptibility and the relative permeability of a co-material placed intimately in contact with it. This is just an engineering feature for easier design.

The author then solves the set of equations in the s-domain[8] for the current as R→0:

$$i(t) = \frac{DM_0}{N}e^{-t/\tau_{ferro}} = \frac{DM_0}{N}e^{-tR/L(1+\mu_r\chi)} \qquad \text{eqn. 30}$$

And calculates the ultimate electrical work delivered to the load $\int_0^\infty i^2(t)R\,dt \Rightarrow$

$$W_{dw.L/R\to\infty} = \frac{1}{2}\frac{\mu_0}{\left(1 + \chi\mu_r\right)}M^2V \qquad \text{eqn. 31}$$

The work done magnetising is given by: $\int HdB \cdot dV$ of which the "H" field energy is discarded, as this can be returned with total efficiency if done by a mechanical magnetisation process or very nearly so with an electronic process ([8] sec. 3.2), leaving:

$$\int_{M,V} \mu_0\mu_r HdM \cdot dV = \mu_0 HM'V$$

The integrand has been resolved with the relative permeability of the material in close proximity to the working substance (the "co-material") subsumed into M'. We can further write the integrand by $M' = \mu_r\chi H$ as (dropping the primes):

$$E_{mag} = \frac{\mu_0}{\chi\mu_r}M^2V \qquad \text{eqn. 32}$$

The dynamical equations can be simulated (or indeed plotted by experiment[8]) and the electrical work plotted against 1/R:
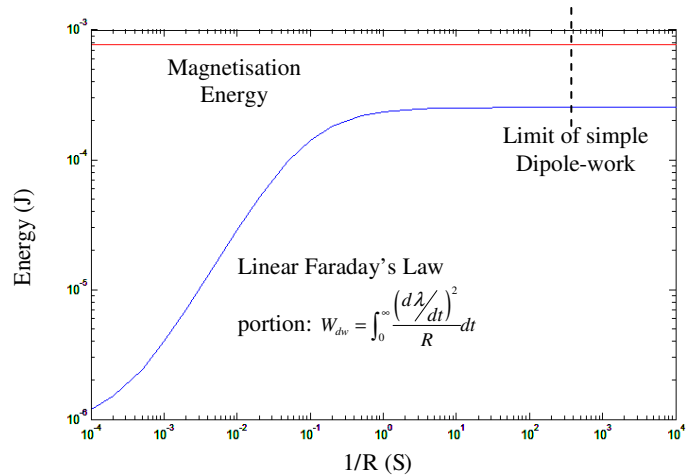

Figure 17 – Magnetisation Energy always exceeds simple dipole-work into resistive load

For the simple arrangement of coil with decaying ferrofluid flux into a resistive load depicted in the lower sub-figure of figure 9, the magnetisation energy input will always exceed the electrical work output. How to circumvent this is discussed in the next section.

2.3.3. The "H-field" cancellation method

The source of the problem for the returned electrical work being less than the magnetisation energy is from the slowing of the current waveforms as the electrical load tends to zero:
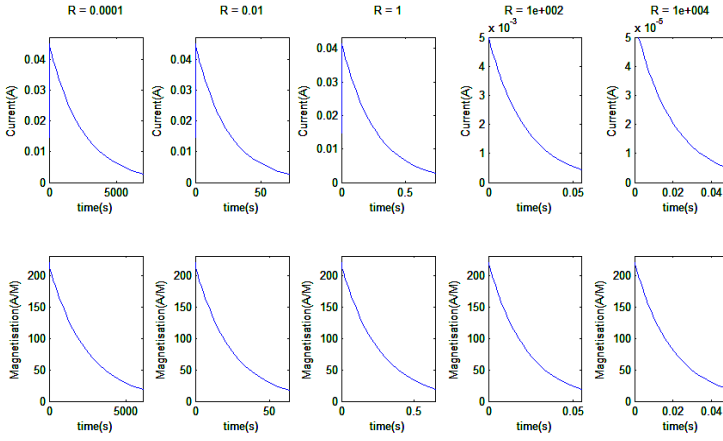

Figure 18 – The slowing current and magnetisation waveforms with lower resistance electrical load

In the s-domain, the current is:

$$I(s) = \frac{\frac{DM_0}{N}}{s^2 \tau_{ferro} + s\left(\frac{R}{L}\tau_{ferro} + (1+\mu_r\chi)\right) + \frac{R}{L}} \quad \text{eqn. 33}$$

The dominant pole of this function shows that the time constant tends to a function purely of the circuit inductance and resistance:

$$s \cong \frac{c}{b} \Rightarrow -\frac{1}{\tau'_{ferro}} = -\frac{1}{\tau_{ferro} + \frac{L(1+\mu_r\chi)}{R}} \quad \text{eqn. 34}$$

The way around this is to strike out the re-magnetising H-field[3, 4] in equation 26:

$$\frac{dM}{dt} = -\frac{1}{\tau}\left(M - \chi\mu_r H\right)$$

Whereupon new current dynamics result:

$$I(s) = \frac{\frac{DM_0}{N}}{s^2 \tau_{ferro} + s\frac{R}{L}\tau_{ferro} + \frac{R}{L}} \quad \text{eqn. 35}$$

The current in the time domain in the limit R→0 is,

$$i(t) = \frac{DM_0}{N}e^{-t/\tau'_{ferro}} = \frac{DM_0}{N}e^{-tR/L} \quad \text{eqn. 36}$$

And then the dipole-work limit by the cancellation method is obtained by $\int_0^\infty i^2(t)Rdt$ once again:

$$W_{dw.cancel.L/R\to\infty} = \frac{1}{2}\mu_0 M^2 V \quad \text{eqn. 37}$$

This is seen to be the magnetic field energy of the ferrofluid flux and is greater than the input magnetising energy, equation 32. Simulating the dynamic equations with the approach[8] one can plot and obtain the graph below for one set of parameters $\chi\mu_r \simeq 30$:
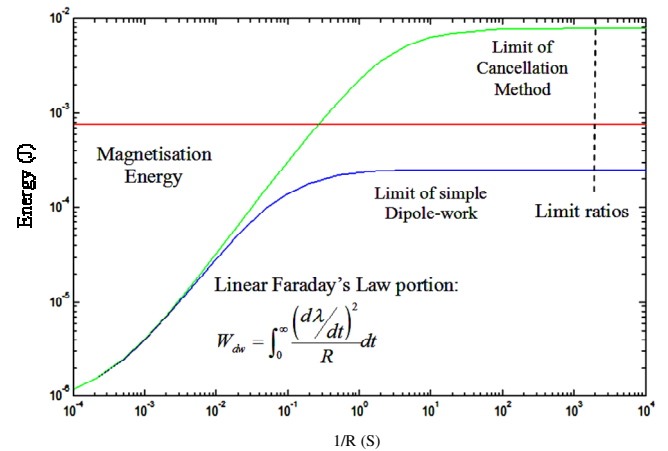

Figure 19 – Dipole-work exceeding magnetisation energy by the H-field cancellation method

We can plot the variation in the limit ratios of the simple dipole-work, the magnetisation energy and the dipole-work with the cancellation method versus parameter $\chi\mu_r$ by taking the ratio of equations 31, 32 and 37:
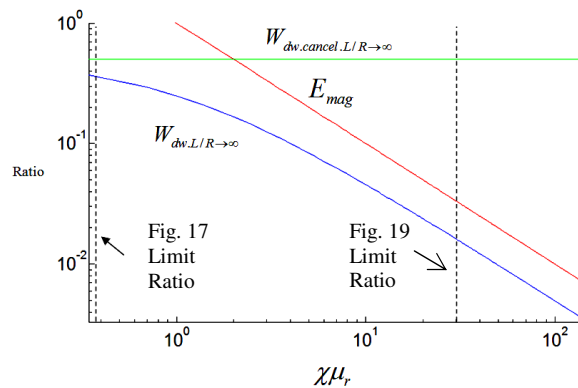

Figure 20 – Variation of parameter $\chi\mu_r$

For all variation of parameters, the magnetisation energy is always greater than the dipole-work without the cancellation method. However if $\chi\mu_r > 2$ the dipole-work, with the cancellation

method, will exceed the magnetisation energy input. The power produced by the device is then:

$$P = \left(W_{dw.cancel} - E_{mag} - W_{losses} \right) F_{cycle}$$

Confirming what was said in the thermodynamic section and equation 16.

The circuit to perform the cancellation method is shown below and detailed description of its mechanism of action can be found in the thesis ([8], sec. 4.3).
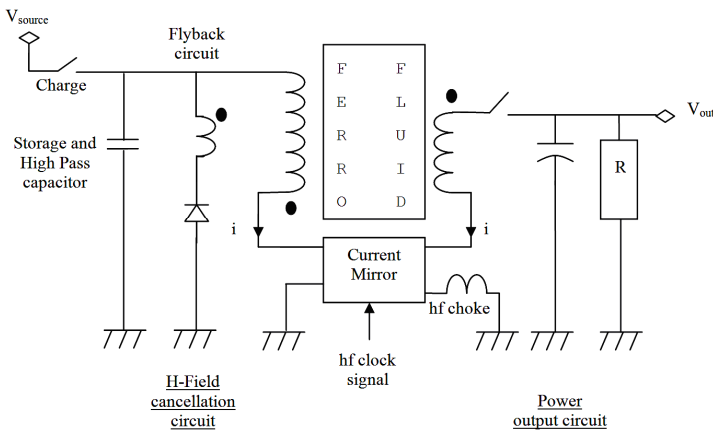

Figure 21 – The H-Field Cancellation Scheme (LHS circuit)

The circuit works by sampling the current in the power circuit (RHS) and makes a "chopped" proportional copy of it.
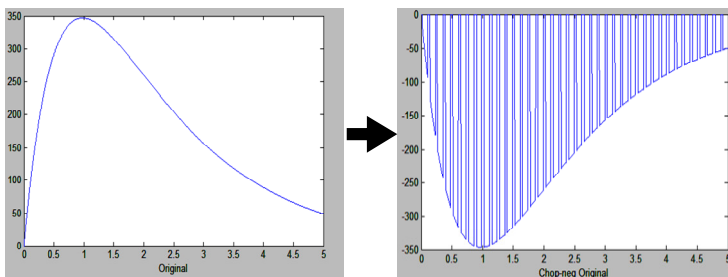

Figure 22 – Sampling, inverting and "chopping" the current/H-field

The LHS then generates its own H-field which sums with the RHS. The ferrofluid naturally low-pass filters this resultant H-field because of its high harmonics and even more so at very high frequency where the ferrofluid will not exhibit a response nor dissipation (fig. 6). One can observe how the resulting H-field is reduced in the rightmost figure.
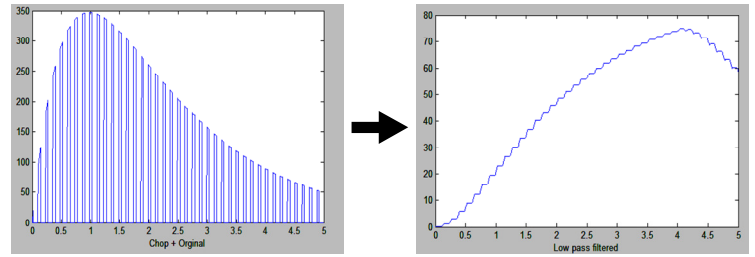

Figure 23 – The resultant high frequency H-field gets low-pass filtered

Even better cancellation comes from asymmetric summation of the inverted, chopped field to the magnetising field. Below is shown the result of summing -1.5 x the original field:
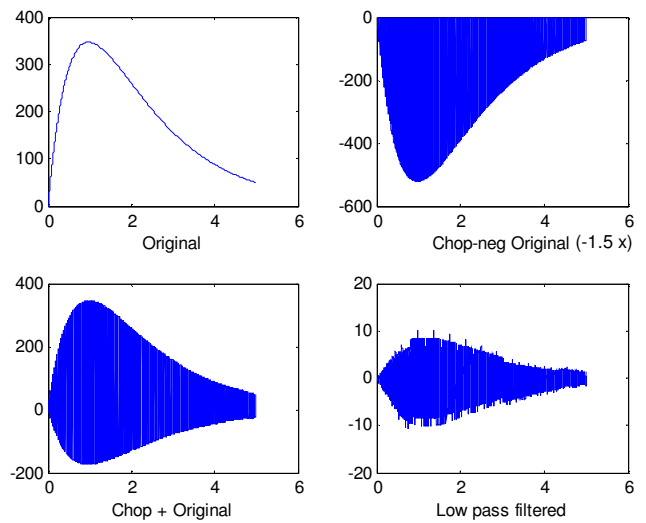

Figure 24 – Asymmetric sampling and summation

The author analyses the electrical work required to operate the H-field cancellation scheme ([8], sec. 4.3.1) and notes that by the inclusion of filtering elements and the "flyback" circuitry, that the LHS circuit only does work establishing the cancellation field and this can be done with high efficiency in a regenerative manner.

3. Conclusion

This paper on the analysis of the Temporary Remnant cycle is built on the foundations of Kinetic Theory, Thermodynamics, Electrodynamics and experiment.

Kinetic Theory shows that the relaxing magnetic field acts as a velocity damping term to each magnetic particle undergoing Brownian motion. The electromagnetic field couples to the thermal system, the electromagnetic system then couples to the external electrical system to which power is transferred.

Thermodynamics shows:

- A "delta T", a change in temperature of the working substance from the magnetic work related to the magnetic properties of the material.

- On considering the magnetic enthalpy[8], a new term "MdM" called the dipole-work is added onto the thermodynamic identity and is only relevant when heat transfer occurs. This happens on the second half of the Temporary Remanence cycle. This ties in with the Kinetic Theory where MdM is the velocity damping term.

- T-S diagrams show how the entropies of the magnetic system form a heat engine. Tying in with Kinetic Theory, once again, the variation in entropy associated with the velocity distribution of the magnetic particles is the source of the heat transference.

- An energy balance equation that shows how the internal energy of the working substance falls with electrical work it performs.

Electrodynamics shows:

- The dynamics of the electrical generation process.

- The work delivered to an electrical load by Faraday/Lenz/Maxwell induction law and that this is of the form MdM, once again.

- The work delivered to an electrical load with the field cancellation technique and that this exceeds the input magnetisation energy substantially. The difference comes from the conversion of heat energy to electrical energy.

Cornwall[8] (2.2.3) shows that power densities at least around 1MW per 1m^3/s flow-rate are possible with the technique and this is comparable to existing heat engines and heat pumps, though high efficiency and few moving parts.

References

1. Jackson, J.D., *Classical Electrodynamics*. 2nd ed. 1975: Wiley.

2. Landau, L., *A Course in Theoretical Physics: Classical Theory of Fields*. Vol. Vol. 2 1982: Butterworth-Heinemann.

3. Feynman, L., Sands, *The Feynman Lectures on Physics*. Addison-Wesley, Reading, Massachusetts. Vol. Vol.1, Vol. 2 1989. 14.7, 15.1-6, 35.4

4. Bozorth, R.M., *Ferromagnetism*. IEEE Press 1978.

5. Aharoni, A., *Introduction to the Theory of Ferromagnetism*. Oxford Science Publications 1996.

6. Kittel C., K.H., *Thermal Physics*. W. H. Freeman and Company, San Francisco. Vol. 2nd ed. 1980.

7. Rosensweig, R.E., *Ferrohydrodynamics*. Cambridge University Press. 1998.

8. Cornwall R. O., *Novel Thermodynamic Cycles involving Ferrofluids displaying Temporary Magnetic Remanence.* http://webspace.qmul.ac.uk/rocornwall/, 2013. http://vixra.org/abs/1311.0078

9. Gschneidner, K.A., Jr.; Pecharsky, V. K., *Recent developments in magnetocaloric materials.* IOP Reports on Progress in Physics, 2005. **68**(6): p. 1479–1539.

10. J. Romero Gómez, R.F.G., A. De Miguel Catoira, M. Romero Gómez, *Magnetocalorific effect: A review of the thermodynamic cycles in magnetic refrigeration.* Renewable and Sustainable Energy Reviews, 2013. **17**: p. 74-82.

11. Landau, L., *A Course in Theoretical Physics: Statistical Physics*. Vol. Vol. 5. 1996: Butterworth Heinemann.

12. Vallejo-Fernandez, O.G., Patel, *Mechanisms of hyperthermia in magnetic nanoparticles.* J. Phys. D: Appl. Phys., 2013. **46**.

13. Fannin, P.C., *A Study of the Complex Susceptibility of Ferrofluids and Rotational Brownian Motion.* Journal of Magnetism and Magnetic Materials, 1987. **65**: p. 279-281

14. Fannin, P.C., *On the Analysis of Complex Susceptibility Data of Ferrofluids.* Journal of Physics D: Applied Physics, 1988. **21**: p. 1035-1036

15.   Landau, L., *A Course in Theoretical Physics: Kinetics*. Vol. Vol. 10. 1981: Butterworth-Heinemann.

16.   Haile J. M., *Molecular Dynamics Simulation*. 1997: John Wiley and Sons.

[†] Feynman in his lecture notes is quite scathing about the term "H-field" which is used by electrical engineers and those working in the magnetics of materials,

"… there is only ever B-field, the magnetic field density … it is a mathematical arrangement to make the equations of magneto-statics come out like electro-statics when we know isolated magnetic poles don't exist by Maxwell's Equations, div B = 0."